Development of a Microfluidic Ion Current Measurement System for Single-Microplastic Detection

Kishimoto, Yuta
Department of Applied Chemistry, Graduate School of Engineering, Kyushu University

Ide, Sachiko
Department of Applied Chemistry, Graduate School of Engineering, Kyushu University

Naito, Toyohiro
Department of Applied Chemistry, Graduate School of Engineering, Kyushu University

Nakashima, Yuta
Faculty of Advanced Science and Technology, Kumamoto University

他

出版情報：Journal of Robotics and Mechatronics. 35 (5), pp.1193-1202, 2023-10-20. Fuji Technology Press
バージョン：

https://doi.org/10.20965/jrm.2023.p1193

Paper:

Development of a Microfluidic Ion Current Measurement System for Single-Microplastic Detection

Yuta Kishimoto*, Sachiko Ide*, Toyohiro Naito*, Yuta Nakashima,***, Yoshitaka Nakanishi**, and Noritada Kaji*,†**

*Department of Applied Chemistry, Graduate School of Engineering, Kyushu University
744 Motooka, Nishi-ku, Fukuoka 819-0395, Japan
E-mail: kaji@cstf.kyushu-u.ac.jp
**Faculty of Advanced Science and Technology, Kumamoto University
2-39-1 Kurokami, Chuo-ku, Kumamoto 860-8555, Japan
***International Research Organization for Advanced Science and Technology, Kumamoto University
2-39-1 Kurokami, Chuo-ku, Kumamoto 860-8555, Japan
†Corresponding author
[Received April 12, 2023; accepted July 7, 2023]

Microplastics (MPs) can adsorb heavy metals and metalloids and may cause a potential health hazard. Precise measurements of their size, shape, composition, and concentration at a single-MP level are important to evaluate their potential toxicity and identify their original source. However, current single-MP analytical methods such as micro-Raman spectroscopy and scanning electron microscopy have low throughput. Therefore, in this study, we applied the ion current sensing method, which has been used for single cell analysis, to single-MP analysis and examined whether size measurement and composition analysis of MPs at the single particle level are possible. In single-MP measurements, plastic particles must be monodispersed in solution at least within the measurement time. The agglomeration behavior was carefully observed after adding sodium dodecyl sulfate to tris-borate-EDTA buffer at 2–16 mM. Under these conditions, the size of polystyrene beads could be measured using the ion current sensing under the monodispersed condition. Next, ion current sensing was performed on four pseudo MPs fabricated from different materials (polyethylene, polyethylene terephthalate, polypropylene, and polyvinyl chloride) that were mechanically grazed and UV-irradiated to imitate real marine MPs. Although significant differences in the ion current signals from different material MPs were not observed, fast (100 MPs within 2 s) and precise measurements in the MPs' sizes at a single-MP level were successfully achieved.

Keywords: microfluidic devices, microplastics, ion current sensing, single microplastic detection

1. Introduction

Owing to the exponential increase in plastic products, the amount of emitted plastic debris in the environment, including microplastics (MPs), which are particles or pieces smaller than 5 mm in diameter, has dramatically increased and is being closely monitored as a significant problem, particularly in marine pollution sources [1–3]. MPs can be classified into two types based on their sources: primary and secondary MPs [4]. Primary MPs are manufactured in the form of particles and are used as scrub agents in toothpaste, facial cleansers, and cosmetics. Secondary MPs are the products that have been crushed and fragmented in the natural environment by physical and chemical processes, such as UV light, heat, and wind waves in marine environments [5]. MPs released into the natural environment through these processes have been reported to cause internal abrasion, obstruction of the gastrointestinal system, and accumulation in the organs of marine organisms through accidental ingestion and the food chain, eventually leading to human health hazards [6–8].

Several techniques such as scanning electron microscopy (SEM), Fourier transform infrared spectroscopy (FT-IR), and Raman spectroscopy have revealed that half of the MPs in the ocean consist of polyethylene (PE) and 30% have diameters smaller than 20 μm [9]. Because MPs ingested by marine organisms are mostly 10 μm or smaller, their accumulation in the body is size-dependent [10]. In addition, ingested MPs penetrate cell membranes and accumulate in the organs [11]. They might be highly toxic not only because of the constituent materials of MPs but also because of the stabilizing agents contained in MPs, UV-degraded chemicals, and adsorbed chemicals, including heavy metals, during fragmentation.

However, several challenges remain; for instance, SEM does not typically provide information in the z-axis direction and thus cannot be used to accurately assess their

three-dimensional shape and volume. Micro-Raman spectroscopy requires approximately 30 min per scanning area, and the scannable area in a single pass is limited to a few hundred square micrometers; therefore, MPs must be prepared to be localized and uniform in the observation area for high-throughput measurements [12]. Therefore, the development of high-throughput analytical methods at the single-MP level to understand the size, shape, and chemical constituents, is an urgent task for assessing future health hazards.

Recently, microfluidic devices have attracted significant interest as high-throughput analytical tools. We developed a high-throughput single cell [13, 14] and particle analysis method [15] for a microfluidic device called ion current sensing on a chip, which combines an improved Coulter counter with a microfluidic device. Slight changes in the electric resistance in the microchannel as particles pass through the sensing area can be detected by monitoring the ion current, enabling us to measure the size of PM2.5, cells, and bacteria [16], which are a few hundred nanometers to a few tens of micrometers in size. The application of this technology to MPs analysis is expected to provide the precise size information of MPs at the single-MP level.

Therefore, in this study, we optimized the system for MP measurements, specifically the detection channel length and the conductive solution, to maximize the sensitivity for a single-MP measurement. Ion current sensing of MPs fabricated from PE, polyethylene terephthalate (PET), polypropylene (PP), and polyvinyl chloride (PVC) with shapes and properties similar to those of marine MPs was performed, and their sizes were evaluated.

2. Materials and Methods

2.1. Standard-Size Bead Preparation for Ion Current Sensing

Monodisperse polystyrene (PS) beads (Polybead® Microspheres, Polysciences, Warrington, PA, USA) with diameters of 10, 6, 4.5, and 3 μm and polydisperse PE beads (Spherical Powder HE-3040, Sumitomo Seika Chemicals Co., Ltd., Osaka, Japan) with a median diameter of 11 μm were used as the standard-size MPs. To confirm the size distribution of the standard MPs, they were observed using an inverted microscope (ECLIPSE Ts2, Nikon Corporation, Tokyo, Japan), and the images were analyzed using ToupView software (Hangzhou ToupTek Photonics Co., Ltd., Zhejiang, China) to measure the diameter.

2.2. Microfluidic Ion Current Sensing System

The microfluidic device used for ion current sensing in this study was designed using computer-aided design (AutoCAD, Autodesk Inc., Tokyo, Japan), and mask blanks (CBL4009Bu-AZP, Clean Surface Technology Co., Ltd., Kanagawa, Japan) were used to draw microfluidic channel patterns using a maskless exposure machine (D-light DL-1000, Nano System Solutions, Okinawa, Japan). After UV exposure, the blank masks were immersed in NMD-3 (Tokyo Ohka Kogyo Co., Ltd., Kawasaki, Japan) for 1 min to remove the exposed area. The mask blanks were then immersed in a chromium etchant solution for 1 min to remove the patterned chromium layer, and the remaining resist was removed using acetone. The fabricated chromium masks were used to fabricate molds for fabricating the PDMS device. SU-8 3025 (Nippon Kayaku Co., Ltd., Tokyo, Japan) was spin-coated onto a silicon wafer with 10-μm thickness. After the substrate was prebaked at 95°C for 10 min, the microfluidic channel pattern was UV-exposed using mask aligners (M-1S, Mikasa Co., Ltd., Tokyo, Japan) through the designed chromium mask. After the exposure, the substrate was post-baked at 95°C for 3 min, and subsequently developed by immersing in 2-acetoxy-1-methoxypropane (Kanto Chemical Co., Ltd., Tokyo, Japan) for 2 min. After the development, the substrate was washed with isopropyl alcohol (FUJIFILM Wako Pure Chemical Corp., Osaka, Japan). After the fabrication of the silicon mold, the height of the molds was measured at three locations, each with a step meter (ET200, Kosaka Laboratory Ltd., Tokyo, Japan). Before the PDMS replica was fabricated, the silicon molds were silanized using trichloro (1H,1H,2H,2H-perfluorooctyl) silane (Sigma-Aldrich, Tokyo, Japan). A PDMS base and curing agent (SILPOT 184, Toray) were mixed at a weight ratio of 10 : 1 and deformed using a planetary stirrer (Awatori Rentarou, AR-100, Shinky Corp., Tokyo, Japan), poured on top of the substrate, further degassed in a desiccator for 1 h, and heated at 65°C for 12 h. After curing, the PDMS was cut out, and holes of 2 and 1.2 mm diameter were punched as reservoirs for the electrodes and the sample inlet and outlet, respectively. The surfaces of the PDMS and glass slides (Matsunami Glass Ind., Ltd., Osaka, Japan) were hydrophilized using plasma irradiation with a plasma current of 35 mA or higher for 45 s (PIB-20, Vacuum Device, Co., Ltd., Ibaraki, Japan). The plasma-irradiated surfaces were bonded and heated at 180°C for 30 s to construct the final microfluidic device.

2.3. Principle of Ion Current Sensing

The microfluidic ion current sensing system was the same as used in other studies [13, 14, 16], which consisted of a microfluidic device, a syringe pump (YSP-202, YMC Co., Ltd., Kyoto, Japan) for sample introduction into the microfluidic device, electrodes, a current measurement circuit, a battery, a programmable current amplifier (CA5351, NF Corp., Yokohama, Japan), a multifunction data acquisition (DAQ) device (USB-6259, National Instruments Corp., Austin, TX), and LabVIEW software on a personal computer for data acquisition and analysis, as shown in **Fig. 1**. The electric circuit shown in **Fig. 1(c)** consisted of an electrophoretic driving circuit from the sample inlet (SI) to the sample outlet (SS) and a bridge circuit for current measurement at the intersection of the microfluidic channel. The bridge circuit had a 1 kΩ resistive element, a battery, and a potentiometer (P13LFL106MAB10, Vishay Intertechnology, Inc.,

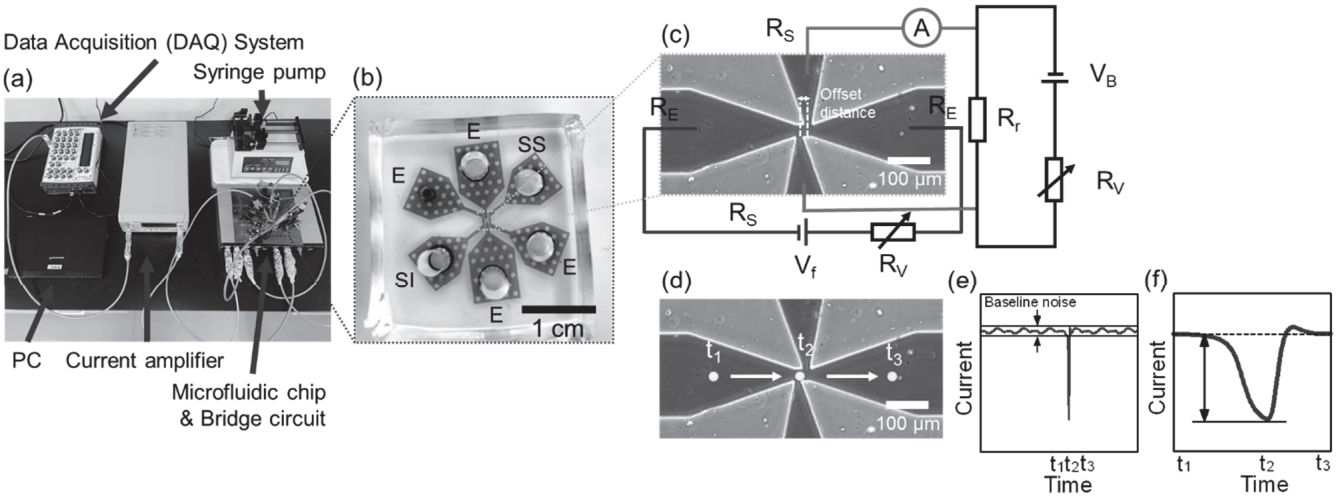

Fig. 1. (a) Overview photo of the microfluidic ion current measurement system. (b) Microfluidic chip filled with a colored dye solution to make the microchannels easy to see. SI: sample introduction reservoir, SS: syringe pump suction reservoir, E: reservoir for electrode. (c) Expanded microscope image of the detection area and the schematic electric circuit. (d)–(f) Working principle of the system. When the microplastic migrates the intersection as shown in (d), a negative current signal appears at time t_2 as shown in (e). (f) Magnified signal around time, t_2, shown in (e). The arrows indicate the signal intensity and correspond to the volume of the microplastics, and the sizes can be estimated.

Malvern, PA) to control the current flow at the detection area for highly sensitive detection. When an MP passed through the detection area, the resistance in the area increased. Thus, a negative signal occurred, as shown in **Fig. 1(d)**. For the MP measurements, the syringe pump was driven at a flow rate of 5 μL/min, and the sampling rate of the DAQ was set to 5 kHz. To confirm that the obtained current signals were derived from the flowing MPs in the detection area, direct observations were performed using an inverted microscope (Axiovert 135 TV, Carl Zeiss, Germany) equipped with a high-speed camera (E-2, Transmedia Research, Spain).

2.4. Conductive Solution for MP Measurements

A 25 × tris-borate EDTA (TBE) buffer solution (pH 8.0) was prepared and diluted with ultrapure water to obtain the desired concentration. Sodium dodecyl sulfate (SDS) (FUJIFILM Wako Pure Chemical Corp., Osaka, Japan) was added to the TBE buffer at concentrations of 2, 4, 8, and 16 mM to avoid the aggregation of microplastics. Conductivity was measured to calculate the resistivity in the microchannel using a conductivity meter (F-54, HORIBA, Kyoto, Japan). Three measurements were taken, and the average value was obtained.

2.5. Evaluation of MP Agglomeration

Because a stable dispersion state in solution should be maintained when measuring MPs at a single-MP level, optimal measurement conditions were investigated based on the agglomeration rate of the PE beads. After the suspension of PE beads at a concentration of 1 mg/mL in TBE buffer with SDS was introduced into the microchannel and maintained for 30 min, the agglomeration of PE beads in the microchannel was directly observed using an optical microscope, and the rate was calculated using the following equation:

$$Agglomeration\ rate = \frac{Agglomerated\ PE\ beads}{Total\ number\ of\ PE\ beads}.$$

2.6. Pseudo-Marine MPs Fabricated from PE, PET, PP, and PVC

Pseudo-marine MPs were produced using a pin-on-disc abrasive machine, as reported in a previous paper [17,18]. Briefly, a pin of 9.0 mm in diameter fabricated from PET, PP, or PVC was pressed onto a quartz glass disc via an air cylinder at a pressure of 2.0 MPa and the fixed pin was subjected to orbital motion with a diameter of 10 mm and a sliding speed of 20.0 mm/s under UV irradiation (UV-B, wavelength of 280–315 nm) and soaked in a saline at approximately 25°C.

3. Results and Discussion

3.1. Device Overview and Ion Current Sensing of MPs

Figure 1(a) shows an overview of the ion current sensing system used in this study. The height of the microfluidic channel was estimated at approximately 14.5 μm according to the mold height fabricated from SU-8. For measurements of MPs smaller than 10 μm, the dimensions of the detection area were optimized for highly sensitive detection. As shown in **Fig. 2**, five different offset distances of 0, 2, 5, 10, and 50 μm were fabricated with 10-μm wide and 14.5-μm high microchannels. The sensitivity of each device was evaluated by using 10 μm PS beads based on the signal-to-noise ratio (S/N). **Fig. 2**

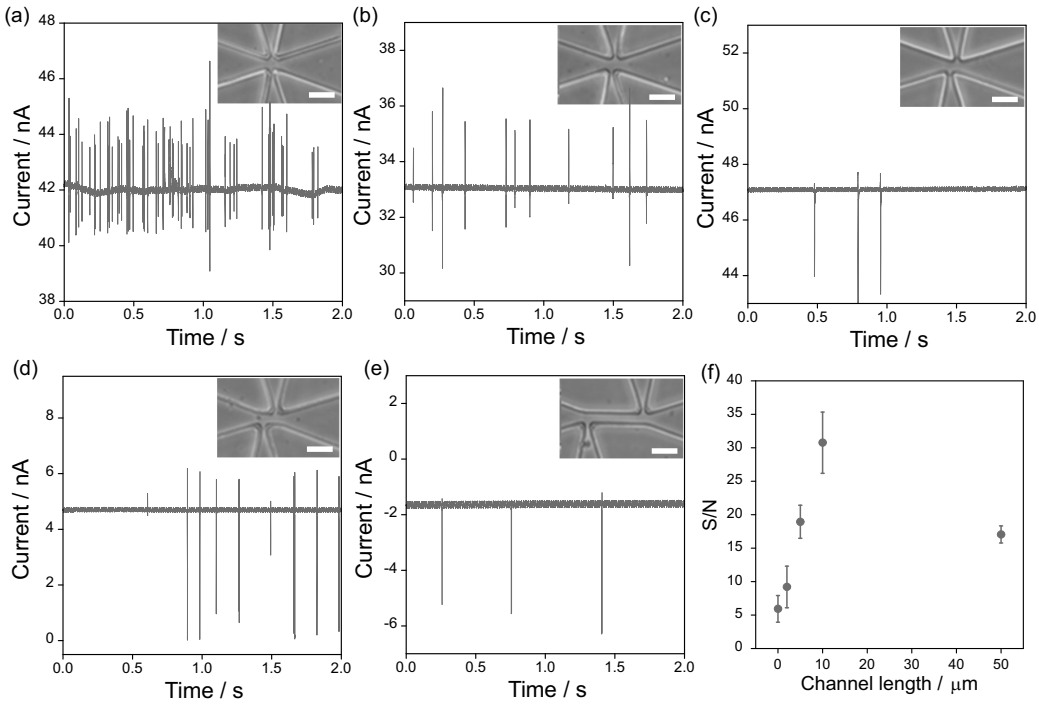

Fig. 2. Typical current signals of 10-μm PS beads in microchannel with offset distances of (a) 0 μm, (b) 2 μm, (c) 5 μm, (d) 10 μm, and (e) 50 μm. The scale bars indicate 20 μm. (f) Signal-to-noise ratios (S/N) as a function of the offset distances.

shows the typical ion current signals of 10-μm PS beads with each device, and the offset distance of 10 μm had the highest sensitivity (**Fig. 2(f)**); therefore, we decided to use the device for further study.

For high-sensitivity detection, the current flow in the detection area was controlled to be as close to 0 A as possible to reduce the thermal noise caused by the current by adjusting the variable resistor (R_v) in the bridge circuit. However, maintaining the current at exactly 0 A for a long period appeared difficult, and it fluctuated slightly, as shown in **Figs. 2** and **5** (described in Sections 3.3 and 3.4). This was inevitable because the liquid functioning as an electrical circuit was only nanoliters in volume, and liquid evaporation from the reservoirs, which could change the conductance of the liquid, cannot be ignored.

Monodisperse PS beads of 10, 6.0, 4.5, and 3.0 μm in diameter and polydisperse PE beads of 11 μm in median diameter were used as standard-size MPs. The size distributions of the polydisperse PE beads were measured based on optical microscope images and the mean, medium, and mode diameter of PE beads were 4.8, 4.4, and 3.5 μm, respectively. The most important aspect of performing a single-particle measurement is to maintain the particles in a dispersed state in the solution during the measurement time. Nanoparticles tend to agglomerate to reduce the surface free energy, and microparticles tend to undergo sedimentation. Therefore, the optimum solution conditions for maintaining the dispersed state were determined by measuring the agglomeration ratio of the polydisperse PE beads. A dedicated device for measuring the agglomeration ratio is shown in **Fig. S1** in Appendix A1. In the TBE buffer solution without SDS,

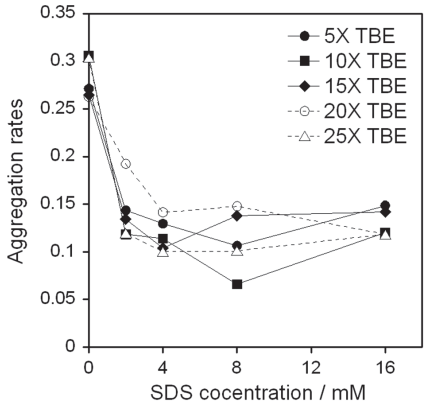

Fig. 3. Agglomeration rates of the high-density polyethylene (HDPE) beads as a function of SDS concentration.

the PE beads began to agglomerate immediately after dispersion in the buffer solution, and after 30 min, almost all the beads formed agglomerates. **Fig. 3** shows the agglomeration rate of the PE beads at different concentrations of SDS and TBE buffers. The results showed that the conductive solution with SDS was effective in dispersing the PE beads, even at a low concentration of SDS (2 mM). However, highly conductive solutions, such as the 25 × TBE buffer, caused the precipitation of crystalline-like materials over time and clogged the detection area, as shown in **Fig. S2** in Appendix A2. This may have been caused by oversaturation accompanying solution evaporation, which elevated the temperature under an applied electric field, particularly in the detection

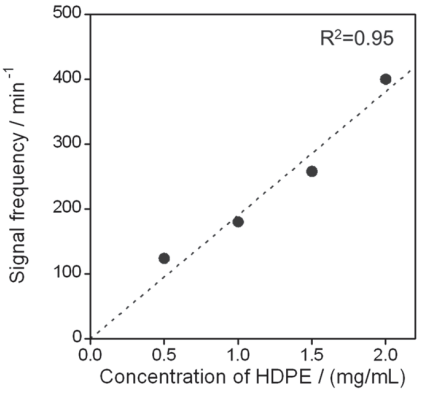

Fig. 4. Current signal frequency as a function of concentration of the HDPE beads.

area where the electric field was concentrated. Therefore, 5 × TBE buffer with 2 mM SDS, which had a relatively low ionic strength of 0.193 S/m at 17.9°C, was used for the subsequent experiments.

3.2. MPs Concentration and Frequency of the Ion Current Signals

To confirm whether the ion signals reflected the passage of MPs in the detection area, we visualized the passage of the PE beads using a high-speed camera. As shown in the movie [a], the passage of the MPs and the migration time were confirmed, and PE bead agglomeration was not observed. To increase the throughput, we measured different concentrations of PE beads under 5 µL/min flow conditions to optimize the sample concentration, and we observed the signal frequency. Because the PE beads were polydisperse, only ion current signals with an S/N greater than 1 were counted. **Fig. 4** shows that the frequency of the ion current signal increased linearly with increasing concentrations of PE beads from 0.5 to 2.0 mg/mL. This result also confirmed that signals derived from the PE beads, no consecutive signals, and MPs clogging in the detection area were observed in this concentration range.

3.3. Theoretical Prediction and Actual Measurement

The detected current signal, i_{signal}, was calculated using the resistance change (ΔR_x) during the MP passage in the detection area. A theoretical estimation of the ion current signals was performed using the following equation:

$$i_{signal} = \frac{V_f}{\alpha} \times \Delta R_x, \quad \ldots\ldots\ldots\ldots (1)$$

$$\alpha = (2R_E + R_x) \times (2R_s + R_x + R_r), \quad \ldots (2)$$

$$R = \rho \frac{L}{W \times H}, \quad \ldots\ldots\ldots\ldots (3)$$

where R_x and V_f are the resistance of the detection area and applied voltage (8.26 V), respectively. R_E, R_s, and R_r are the resistances of the electrophoretic channel, sensing channel, and resistive element of 1 kΩ in the bridge circuit, respectively. ρ, W, H, and L are the conductivity of the solution (5.18 Ω·m), the width (10 µm), the height (14.5 µm), and the length (10 µm) of the detection area, respectively. When PS beads of 3, 4.5, 6, and 10 µm in diameter migrated to the detection area, i_{signal} was calculated as 0.35, 1.2, 2.9, and 20 nA, respectively.

Various sizes of PS beads were measured, as shown in **Figs. 5(a)–(d)**, and the size dependence of signal intensities exhibited a trend similar to that predicted by the theoretical calculations, as shown in **Fig. 5(e)**. Although the actual measured values were approximately half of the theoretical values, this is understandable from the perspective of local Joule heating at the detection area and a rough estimation of the microfluidic channel volume associated with the positional error of the electrodes in the reservoirs.

3.4. Ion Current Sensing of Pseudo Marine MPs

Frictionally grazed PE, PET, PP, and PVC were used as model MPs with sizes, shapes, and chemical compositions similar to those of actual marine MPs. The similarity of these MPs to those in the environment was adequately verified in a previous report through visual inspection, aspect ratios, and complexity [18]. As shown in **Fig. S3** in Appendix A3, these pseudo-marine MPs were detected using the ion current sensing system, and various signal intensities were observed. These results indicated the polydispersity of pseudo-marine MPs in terms of their size and shape. Because spherical-size-defined beads fabricated from PET, PP, and PVC were not available, the calibration curve obtained for the PE beads, shown in **Fig. 5(e)**, was applied to estimate their sizes. As a result, as shown in **Fig. 6(e)**, the mean diameters of the frictionally grazed PE, PET, PP, and PVC were 3.96, 3.58, 3.46, and 3.41 µm, respectively, assuming a spherical shape. In contrast, under the same assumption, the median diameters of frictionally grazed PE, PET, PP, and PVC were 3.50, 2.99, 3.33, and 3.16 µm, respectively. Outliers above the highest values observed for PE, PET, and PVC are common in this type of top-down microparticle fabrication, whereas outliers below the lowest values were not observed because of the limited sensitivity of the system. A possible reason for the different size distributions is the different shapes of the MPs, particularly the aspect ratio and complexity, which have been extensively studied in a previous study [18]. In the MPs fabricated from PE, which exhibited the largest size distribution, the aspect ratio and complexity were the largest; thus, volume sensing by ionic current might be overestimated because the hydrodynamic radius is larger than the same volume of MPs, which have a low aspect ratio and complexity. Another possible reason could be that the material caused different thicknesses of the hydration layer on the surface of the MPs, depending on the hydrophobicity. Although determining the shape and material composition from the ion current signals remains a challenge, this simple operation and high-throughput method, approximately 100 MPs/min, can provide a new method for single-MP analysis.

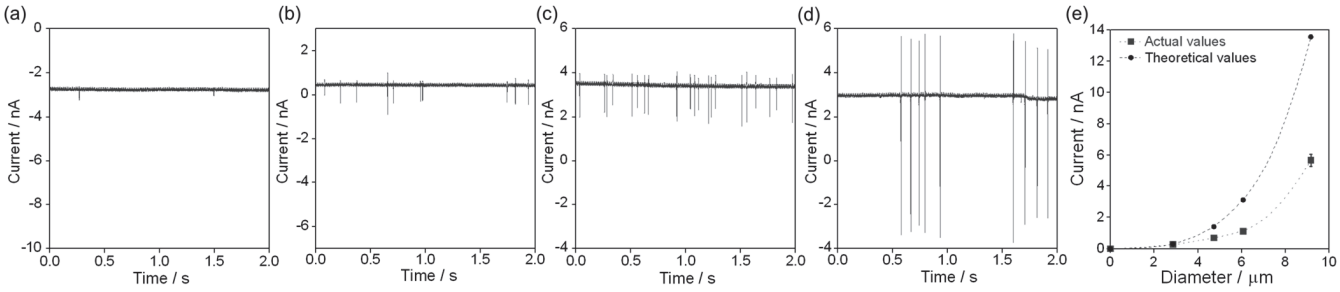

Fig. 5. Typical current signals generated by the passage of (a) 3 μm, (b) 4.5 μm, (c) 6 μm, and (d) 10 μm PS beads in a 10-μm detection length. (e) Current signal plots of actual values and theoretical prediction as a function of PS-bead diameter. The standard deviation of the actual values ($n = 10$) were relatively small and overlapped with the plots.

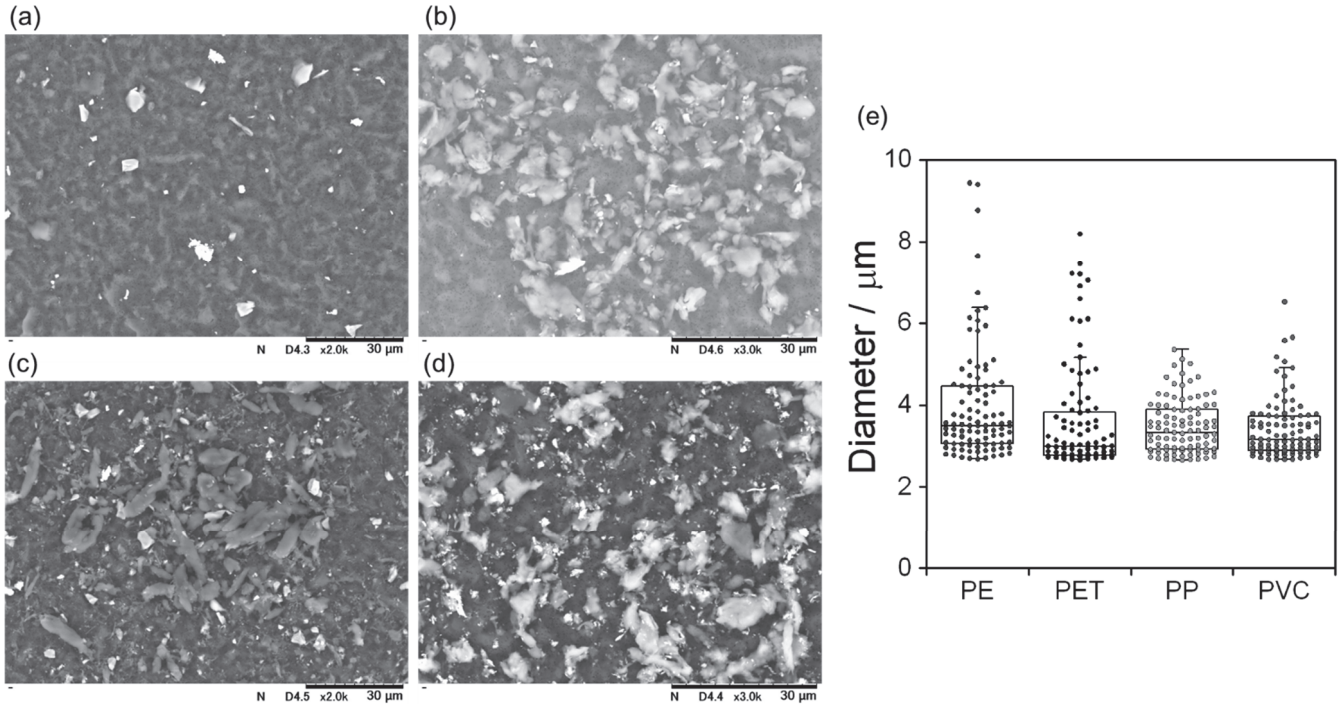

Fig. 6. SEM images of the pseudo-marine MPs produced by a pin-on-disc abrasive machine [17, 18]. The materials were fabricated from (a) PE, (b) PET, (c) PP, and (d) PVC. (e) Box plot overlaid with dot plot of the mean diameter of the pseudo-MPs estimated from the calibration curve shown in **Fig. 5(e)** on the assumption of spherical shape.

4. Conclusion

In this study, we established a method of evaluating MPs smaller than 10 μm at a single-MP level by optimizing a microfluidic ion current sensing system considering the detection channel length, conductive solution preventing MPs agglomeration, and concentration for higher sensitivity and throughput detection. Although the ion current signals detected using standard MP samples had a lower intensity than the theoretical prediction, the size dependence of the calibration curve was the same and available for MP sizing. Pseudo-marine MPs fabricated from PE, PET, PP, and PVC were also measured using a sensing system, and their sizes were estimated under the assumption of a spherical shape. Although the obtained current signal, including the signal intensity, area, and shape, may contain the size, shape, and material information, further investigation using information technology such as machine learning is required to explore the identification of pseudo-marine MPs at the level of individual MPs.

Acknowledgments

This work was partially supported by JST Grant Number JPMJPF2107 and JSPS KAKENHI Grant Numbers JP19KK0140 and 21H01966.

References:

[1] A. L. Andrady, "Microplastics in the marine environment," Marine Pollution Bulletin, Vol.62, Issue 8, pp. 1596-1605, 2011. https://doi.org/10.1016/j.marpolbul.2011.05.030
[2] H. Yang, G. Chen, and J. Wang, "Microplastics in the Marine Environment: Sources, Fates, Impacts and Microbial Degradation," Toxics, Vol.9, No.2, Article No.41, 2021. https://doi.org/10.3390/toxics9020041
[3] X. Guo and J. Wang, "The chemical behaviors of microplastics in

marine environment: A review," Marine Pollution Bulletin, Vol.142, pp. 1-14, 2019. https://doi.org/10.1016/j.marpolbul.2019.03.019

[4] M. Cole, P. Lindeque, C. Halsband, and T. S. Galloway, "Microplastics as contaminants in the marine environment: A review," Marine Pollution Bulletin, Vol.62, Issue 12, pp. 2588-2597, 2011. https://doi.org/10.1016/j.marpolbul.2011.09.025

[5] S. M. Praveena, S. N. M. Shaifuddin, and S. Akizuki, "Exploration of microplastics from personal care and cosmetic products and its estimated emissions to marine environment: An evidence from Malaysia," Marine Pollution Bulletin, Vol.136, pp. 135-140, 2018. https://doi.org/10.1016/j.marpolbul.2018.09.012

[6] C. M. Rochman, M. A. Browne, B. S. Halpern, B. T. Hentschel, E. Hoh, H. K. Karapanagioti, L. M. Rios-Mendoza, H. Takada, S. Teh, and R. C. Thompson, "Classify plastic waste as hazardous," Nature, Vol.494, No.7436, pp. 169-171, 2013. https://doi.org/10.1038/494169a

[7] V. Stock, L. Böhmert, E. Lisicki, R. Block, J. Cara-Carmona, L. K. Pack, R. Selb, D. Lichtenstein, L. Voss, C. J. Henderson, E. Zabinsky, H. Sieg, A. Braeuning, and A. Lampen, "Uptake and effects of orally ingested polystyrene microplastic particles in vitro and in vivo," Archives of Toxicology, Vol.93, No.7, pp. 1817-1833, 2019. https://doi.org/10.1007/s00204-019-02478-7

[8] S. E. Nelms, T. S. Galloway, B. J. Godley, D. S. Jarvis, and P. K. Lindeque, "Investigating microplastic trophic transfer in marine top predators," Environmental Pollution, Vol.238, pp. 999-1007, 2018. https://doi.org/10.1016/j.envpol.2018.02.016

[9] D. Schymanski, C. Goldbeck, H.-U. Humpf, and P. Fürst, "Analysis of microplastics in water by micro-Raman spectroscopy: Release of plastic particles from different packaging into mineral water," Water Research, Vol.129, pp. 154-162, 2018. https://doi.org/10.1016/j.watres.2017.11.011

[10] M. Cole, P. Lindeque, E. Fileman, C. Halsband, R. Goodhead, J. Moger, and T. S. Galloway, "Microplastic Ingestion by Zooplankton," Environmental Science & Technology, Vol.47, No.12, pp. 6646-6655, 2013. https://doi.org/10.1021/es400663f

[11] A. Karami, N. Romano, T. Galloway, and H. Hamzah, "Virgin microplastics cause toxicity and modulate the impacts of phenanthrene on biomarker responses in African catfish (Clarias gariepinus)," Environmental Research, Vol.151, pp. 58-70, 2016. https://doi.org/10.1016/j.envres.2016.07.024

[12] A. M. Elert, R. Becker, E. Duemichen, P. Eisentraut, J. Falkenhagen, H. Sturm, and U. Braun, "Comparison of different methods for MP detection: What can we learn from them, and why asking the right question before measurements matters?," Environmental Pollution, Vol.231, Part 2, pp. 1256-1264, 2017. https://doi.org/10.1016/j.envpol.2017.08.074

[13] M. Sano, N. Kaji, Q. Wu, T. Naito, T. Yasui, M. Taniguchi, T. Kawai, and Y. Baba, "Quantitative Evaluation of Dielectric Breakdown of Silicon Micro- and Nanofluidic Devices for Electrophoretic Transport of a Single DNA Molecule," Micromachines-Basel, Vol.9, Issue 4, Article No.180, 2018. https://doi.org/10.3390/mi9040180

[14] M. Terada, S. Ide, T. Naito, N. Kimura, M. Matsusaki, and N. Kaji, "Label-free cancer stem-like cell assay conducted at a single cell level using microfluidic mechanotyping devices," Anal. Chem., Vol.93, No.43, pp. 14409-14416, 2021. https://doi.org/10.1021/acs.analchem.1c02316

[15] T. Shimada, H. Yasaki, T. Yasui, T. Yanagida, N. Kaji, M. Kanai, K. Nagashima, T. Kawai, and Y. Baba, "PM2.5 Particle Detection in a Microfluidic Device by Using Ionic Current Sensing," Analytical Sciences, Vol.34, No.12, pp. 1347-1349, 2018. https://doi.org/10.2116/analsci.18C018

[16] H. Yasaki, T. Yasui, T. Yanagida, N. Kaji, M. Kanai, K. Nagashima, T. Kawai, and Y. Baba, "Substantial Expansion of Detectable Size Range in Ionic Current Sensing through Pores by Using a Microfluidic Bridge Circuit," J. Am. Chem. Soc., Vol.139, No.40, pp. 14137-14142, 2017. https://doi.org/10.1021/jacs.7b06440

[17] Y. Nakanishi, H. Yamaguchi, Y. Hirata, Y. Nakashima, and Y. Fujiwara, "Micro-abrasive glass surface for producing microplastics for biological tests," Wear, Vol.477, Article No.203816, 2021. https://doi.org/10.1016/j.wear.2021.203816

[18] Y. Nakanishi, Y. Fujiwara, and Y. Nakashima, "Generation of Nano/Microplastics for Immunological Assessments," Biotribology, Vols.33-34, Article No.100235, 2023. https://doi.org/10.1016/j.biotri.2023.100235

Supporting Online Materials:

[a] Movie S1: The behavior of the individual PE beads at the detection area captured by the high-speed camera. No agglomeration was confirmed. The movie is $1/10\times$ playback speed. https://drive.google.com/file/d/1QfnI0d6kWVrsabrz8y0rsVoY3tdhmwTZ/view [Accessed June 22, 2023]

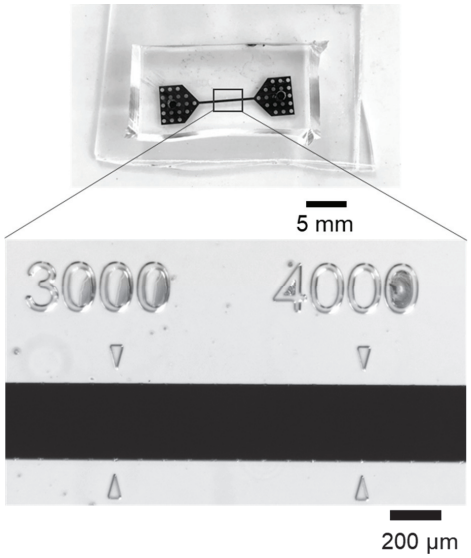

Fig. S1. Dedicated device for measuring the agglomeration ratio of HDPE beads. The microchannel was filled with a dye solution to make it easier to see.

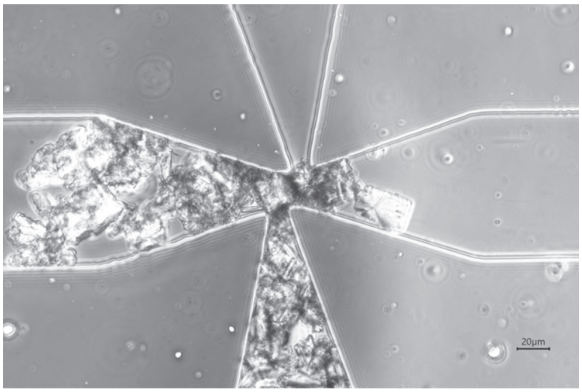

Fig. S2. Typical precipitation images of crystalline-like materials over time at the detection area under ionic current sensing in a relatively high conductive buffer such as $25\times$ TBE. When the conductive solutions precipitated and clogged the microchannel, no further sensing could be performed.

Appendix A.

A.1.

To optimize the solution conditions to maintain the dispersed state of the polydisperse PE beads in the microchannel, we fabricated a dedicated device and measured the agglomeration ratio (**Fig. S1**).

A.2.

The conductive solution with SDS was effective in dispersing the PE beads, even at a low concentration of SDS (2 mM). However, highly conductive solutions such as $25\times$ TBE buffer caused the precipitation of crystalline-like materials over time and clogged the detection area (**Fig. S2**).

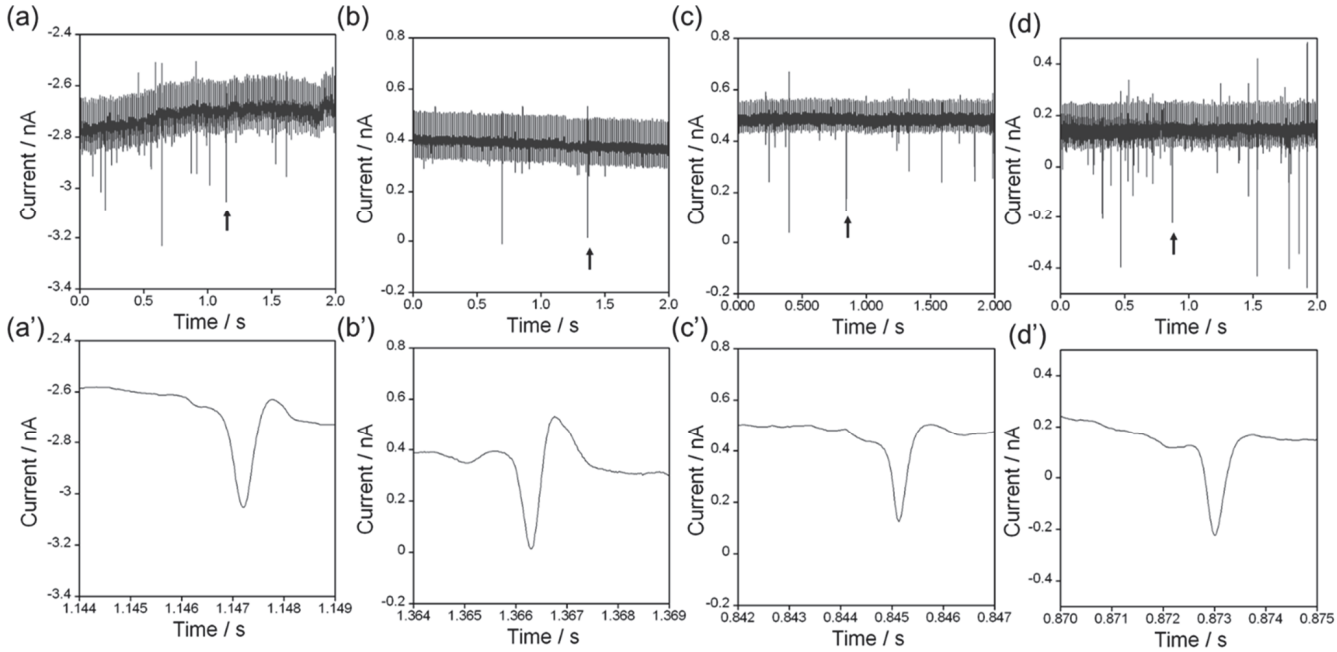

Fig. S3. Typical current signals generated by the pseudo-marine MPs created from (a) PE, (b) PET, (c) PP, (d) PVC in a 10-μm detection length. (a′)–(d′) are the magnified signals indicated by arrows in (a)–(d), respectively.

A.3.

The pseudo-marine MPs were detected using the ion current sensing system, and various signal intensities were observed (**Fig. S3**).

Name:
Yuta Kishimoto

Affiliation:
Graduate Student, Department of Applied Chemistry, Graduate School of Engineering, Kyushu University

Address:
744 Motooka, Nishi-ku, Fukuoka 819-0395, Japan

Brief Biographical History:
2017-2020 Department of Applied Chemistry, School of Engineering, Kyushu University
2021-2022 Department of Applied Chemistry, Graduate School of Engineering, Kyushu University
2023- Morinaga Milk Industry Co., Ltd.

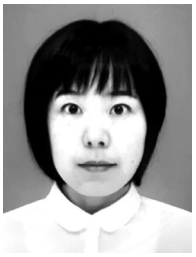

Name:
Sachiko Ide

Affiliation:
Technical Staff, Department of Applied Chemistry, Faculty of Engineering, Kyushu University

Address:
744 Motooka, Nishi-ku, Fukuoka 819-0395, Japan

Brief Biographical History:
2012- Kumamoto Institute of Total Fitness
2016- Senju Pharmaceutical Co., Ltd.
2018- Kyushu University

Main Works:
• "Quantitative Evaluation of Interleukin-4 by Immunowall Devices Made of Gelatin Methacryloyl Hydrogel," Molecules, Vol.28, Article No.4635, 2023.
• "Antioxidants encapsulated milk-derived exosomes for functional food development," Analytical Sciences, Vol.39, pp. 705-712, 2023.
• "Label-free cancer stem-like cell assay conducted at a single cell level using microfluidic mechanotyping devices," Analytical Chemistry, Vol.93, pp. 14409-14416, 2021.

Name:
Toyohiro Naito

ORCID:
0000-0002-9828-873X

Affiliation:
Assistant Professor, Department of Applied Chemistry, Graduate School of Engineering, Kyushu University

Address:
744 Motooka, Nishi-ku, Fukuoka 819-0395, Japan

Brief Biographical History:
2013- Assistant Professor, Department of Material Chemistry, Graduate School of Engineering, Kyoto University
2020- Assistant Professor, Department of Applied Chemistry, Graduate School of Engineering, Kyushu University
2022- Riken Innovation Co., Ltd.

Main Works:
• "Development of a microfluidic dispensing device for multivariate data acquisition and application in molecularly imprinting hydrogel preparation," J. Mater. Chem. B, Vol.10, pp. 6664-6672, 2022.
• "Fluorescent detection of target proteins via a molecularly imprinted hydrogel," Analytical Methods, Vol.13, pp. 3086-3091, 2021.
• "Simple chemical detection based on a surface-modified electroosmotic pump via interval immobilization," Analytical Methods, Vol.13, pp. 1559-1564, 2021.
• "Separation of saccharides using fullerene-bonded silica monolithic columns via π interactions in liquid chromatography," Scientific Reports, Vol.10, Article No.13850, 2020.
• "Controllable molecular sieving by copoly(poly(ethylene glycol) acrylate/poly(ethylene glycol) diacrylate) based hydrogels via capillary electrophoresis for DNA fragments," ACS Applied Polymer Materials, Vol.2, pp. 3886-3893, 2020.

Membership in Academic Societies:
• The Japan Society for Analytical Chemistry (JSAC)
• The Chemical Society of Japan (CSJ)
• Society for Chemistry and Micro-Nano Systems (CHEMINAS)

Name:
Yuta Nakashima

ORCID:
0000-0003-3151-4963

Affiliation:
Associate Professor, Faculty of Advanced Science and Technology, Kumamoto University

Address:
2-39-1 Kurokami, Chuo-ku, Kumamoto 860-8555, Japan

Brief Biographical History:
2007- Postdoctoral Fellow, Graduate School of Life Science and System Engineering, Kyushu Institute of Technology
2009- Assistant Professor, Graduate School of Medicine, Yamaguchi University
2013- Assistant Professor, Graduate School of Science and Technology, Kumamoto University
2015- Associate Professor, Faculty of Advanced Science and Technology, Kumamoto University
2019- Associate Professor, International Research Organization for Advanced Science and Technology, Kumamoto University

Main Works:
• "Evaluation of osteoblastic cell behavior upon culture on titanium substrates photo-functionalized by vacuum ultra-violet treatment," Experimental Cell Research, Vol.410, Article No.112944, 2022.
• "Detection of cancer cells in whole blood using a dynamic deformable microfilter and a nucleic acid aptamer," Talanta, Vol.228, Article No.122239, 2021.
• "A dynamically deformable microfilter for selective separation of specific substances in microfluidics," Biomicrofluidics, Vol.14, Article No.064113, 2020.
• "Method for measuring Young's modulus of cells using a cell compression microdevice," Int. J. of Engineering Science, Vol.114, pp. 41-48, 2017.
• "Creation of cell micropatterns using a newly developed gel micromachining technique," Biofabrication, Vol.8, Article No.035006, 2016.

Membership in Academic Societies:
• The Japan Society of Mechanical Engineers (JSME)
• Society for Chemistry and Micro-Nano Systems (CHEMINAS)
• The Institute of Electrical Engineers of Japan (IEEJ)
• Japanese Cancer Association (JCA)

Name:
Yoshitaka Nakanishi

ORCID:
0000-0002-7975-3595

Affiliation:
Professor, Faculty of Advanced Science and Technology, Kumamoto University

Address:
2-39-1 Kurokami, Chuo-ku, Kumamoto 860-8555, Japan

Brief Biographical History:
1996- JSPS Postdoctoral Fellow, Japan Society for the Promotion of Science
1998- Research Assistant, Kyushu University
1998- Assistant Professor, Faculty of Engineering, Kyushu University
1999- Lecturer, Faculty of Engineering, Oita University
2002- Associate Professor, Faculty of Engineering, Oita University
2004- Associate Professor, Faculty of Engineering, Kyushu Sangyo University
2005- Professor, Department of Digital Medicine Initiative, Kyushu University
2008- Professor, Graduate School of Science and Technology, Kumamoto University
2016- Professor, Faculty of Advanced Science and Technology, Kumamoto University

Main Works:
• "Friction control of elastic materials on glass by means of textured surfaces," Scientific Reports, Vol.12, Article No.15423, 2022.
• "Fabrication of Three-Dimensionally Deformable Metal Structures Using Precision Electroforming," Micromachines, Vol.13, Article No.1046, 2022.
• "A thermoresponsive valve to control fluid flow in microfluidic paper-based devices," Microfluidics and Nanofluidics, Vol.26, Article No.47, 2022.
• "Evaluation of osteoblastic cell behavior upon culture on titanium substrates photo-functionalized by vacuum ultra-violet treatment," Experimental Cell Research, Vol.410, Article No.112944, 2022.
• "Culture System for a Closer Biological Contact Between Macrophages and Microparticles," Frontiers in Mechanical Engineering, Vol.7, Article No.631128, 2021.

Membership in Academic Societies:
• The Japan Society of Mechanical Engineers (JSME)
• Japanese Society for Clinical Biomechanics (JSCB)
• Japanese Society for Musculoskeletal Medicine (JSMM)
• Society of Biomechanisms Japan (SOBIM)
• Japanese Society for Medical and Biological Engineering (JSMBE)
• Japan Society of Computer Aided Surgery (JSCAS)

Name:
Noritada Kaji

ORCID:
0000-0002-9828-873X

Affiliation:
Professor, Department of Applied Chemistry, Graduate School of Engineering, Kyushu University

Address:
744 Motooka, Nishi-ku, Fukuoka 819-0395, Japan

Brief Biographical History:
2005-2011 Assistant Professor, Department of Applied Chemistry, Graduate School of Engineering, Nagoya University
2011-2017 Associate Professor, Department of Applied Chemistry, Graduate School of Engineering, Nagoya University
2018- Professor, Department of Applied Chemistry, Graduate School of Engineering, Kyushu University

Main Works:
• "Quantitative Evaluation of Interleukin-4 by Immunowall Devices Made of Gelatin Methacryloyl Hydrogel," Molecules, Vol.28, Article No.4635, 2023.
• "Antioxidants encapsulated milk-derived exosomes for functional food development," Analytical Sciences, Vol.39, pp. 705-712, 2023.
• "Enzyme kinetics in confined geometries at a single enzyme level," Analyst, Vol.147, pp. 1375-1384, 2022.
• "Label-free cancer stem-like cell assay conducted at a single cell level using microfluidic mechanotyping devices," Analytical Chemistry, Vol.93, pp. 14409-14416, 2021.
• "Observation of ethanol-induced condensation and decondensation processes at a single DNA molecular level in microfluidic devices equipped with a rapid solution exchange system," Analytical Chemistry, Vol.92, pp. 9132-9137, 2020.

Membership in Academic Societies:
• The Japan Society for Analytical Chemistry (JSAC)
• The Chemical Society of Japan (CSJ)
• Society for Chemistry and Micro-Nano Systems (CHEMINAS)